Zeitschrift: IABSE publications = Mémoires AIPC = IVBH Abhandlungen
Band: 31 (1971)

Artikel: A514 steel beam-columns
Autor: Yu, C.K. / Tall, L.
DOI: https://doi.org/10.5169/seals-24224

A 514 Steel Beam-Columns

Colonnes en acier A 514

A 514 Stahl-Stützen

C. K. YU L. TALL
Fritz Engineering Laboratory, Department of Civil Engineering, Lehigh University, Bethlehem, Pennsylvania

1. Introduction

The term beam-column denotes a member which is subject simultaneously to axial thrust and bending. The bending moment in the member may be caused by externally applied end moments, eccentricity of longitudinal forces, initial out-of-straightness of axially loaded columns, or transverse forces in addition to axial forces and end moments. The types of beam-columns which are subject to constant axial force and varying end moments are investigated in this study. The beam-columns studied are assumed to be laterally supported, that is, they fail in the bending plane without twisting.

The determination of the ultimate strength of a beam-column is a problem in which inelastic action must be considered. Extensive research has been carried out in the study of the behavior of laterally supported wide-flange shapes under combined moment and axial force, including the effect of residual stresses [1], [2], [3], [4], [5]. The methods and solutions previously developed are applicable only to materials which have an elastic-perfectly-plastic stress-strain relationship and are restricted to residual stress patterns resulting from cooling after hot rolling of A 36 steel shapes.

Both rolled heat-treated and welded built-up USS T-1 steel shapes are considered in this study. To be exact, A 514 steel does not cover hot-rolled and heat-treated steel shapes. However, hot-rolled and heat-treated T-1 steel shapes have tensile and chemical requirements similar to those of A 514 steel, and therefore, for simplicity, rolled heat-treated T-1 steel shapes are classified here as A 514 steel shapes. The ultimate strength, the load-deformation behavior and the local buckling phenomenon of the beam-columns are investi-

gated. The discussion includes strain reversal and unloading effects. The theoretical analysis is compared with full scale experiments, and the comparison indicates a good correlation.

The purpose of this report is to investigate the strength of both welded and rolled beam-columns made of A 514 steel, and to present a solution to the overall load-deformation characteristics of "non-linear" material including the consideration of strain reversal and unloading.

Stress-Strain Relationship

The stress-strain curve for A 514 steel can be described by the following three Eqs. [6]:

$$\frac{\sigma}{\sigma_y} = \frac{\epsilon}{\epsilon_y}, \quad \text{when} \quad \sigma \leqq \frac{\sigma}{\sigma_y} \leqq 0.8, \tag{1}$$

$$\frac{\sigma}{\sigma_y} = 1.0 + 0.005\left(\frac{\epsilon}{\epsilon_y} - 1.517\right) + 0.3647\left(\frac{\epsilon}{\epsilon_y} - 1.517\right)^3 + 0.3276\left(\frac{\epsilon}{\epsilon_y} - 1.517\right)^5, \tag{2}$$

$$\text{when} \quad 0.8 \leqq \frac{\sigma}{\sigma_y} \leqq 1.0$$

and

$$\frac{\sigma}{\sigma_y} = 1.0 + 0.005\left(\frac{\epsilon}{\epsilon_y} - 1.517\right), \quad \text{when} \quad \frac{\sigma}{\sigma_y} \geqq 1.0, \tag{3}$$

in which σ is stress, σ_y is the yield stress determined by the 0.2% offset method [7], ϵ is strain, and ϵ_y is the yield strain ($= \sigma_y/\epsilon$). Fig. 1 shows the complete stress-strain curve for A 514 steel. By comparing this to that for mild steel,

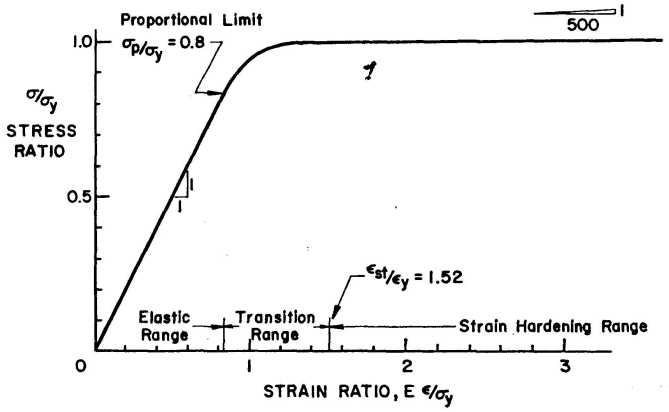

Fig. 1. Typical Stress-Strain Curve for A 514 Steel.

it is seen that A 514 steel has a lower proportional limit stress and that strain hardening occurs immediately after the ending of the transition range, continues until the tensile strength is reached, and then starts to unload. This representative stress-strain curve for A 514 steel was determined by averaging the results of 58 standard ASTM tension specimen tests. The average values of yield stress, modulus of elasticity and strain hardening modulus are 112 ksi,

28,900 ksi and 144 ksi, respectively. (The modulus of elasticity given here is the average value measured directly from the autographically recorded stress-strain curves.)

Residual Stress

Fig. 2 shows the idealized patterns of residual stress distribution in heat-treated rolled *WF* shapes and welded *H*-shapes with flame-cut plates, all of A 514 steel. These idealized patterns are approximation of the results obtained from an extensive investigation on the residual stresses in A 514 steel shapes and plates [8], [9], [10]. For rolles shapes, previous investigation [10] indicates

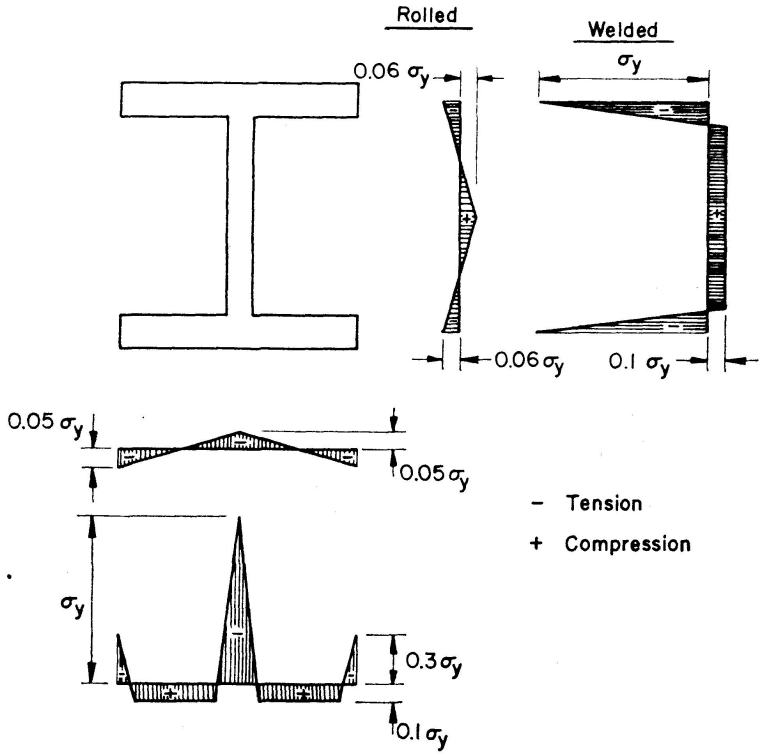

Fig. 2. Idealized Average Residual Stress Distribution in A 514 Steel Shapes.

that the magnitude and pattern of residual stresses essentially are independent of the yield stress of the steel if steel is not heat-treated after rolling. Heat-treatment apparently reduces the residual stress magnitudes as, for example, in rolled A 514 steel shapes. Furthermore, because of the high yield stress of the steel, the residual stress magnitude in rolled A 514 steel, if compared on a nondimensionalized basis with respect to its yield stress, is much smaller than that for structural carbon steels. Thus, the effect of residual stress could be less for rolled A 514 steel beam-columns than for those of A 36 steel. For welded *H*-shapes, the flame-cutting of the component plates creates tensile residual stress at the cut edges; this pattern of residual stress distribution is completely different from that in rolled shapes. Therefore, a separate and different analysis for both rolled and welded shapes of A 514 steel is needed.

Assumptions

The assumptions made in the theoretical analysis are as follows:

1. The members are perfectly straight.
2. The effect of shear is insignificant and can be neglected.
3. The thrust is applied first and then kept constant as the end moments increase or decrease.
4. The members are bent with respect to strong axis and weak axis buckling and lateral-torsional buckling is effectively prevented.

2. Moment - Curvature - Thrust Relationship

Basic Concepts

A prerequisite to performing ultimate strength analyses of beam-columns is a knowledge of the relationship existing between the bending moment and the axial force acting on the cross-section, and the resulting curvature.

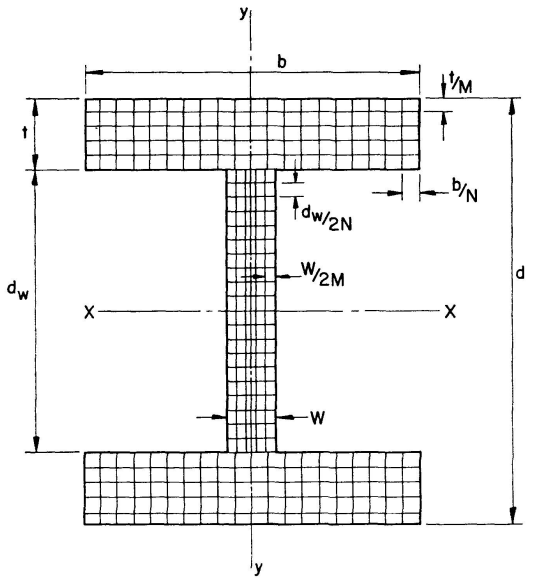

Fig. 3. Arrangement of Finite Area Elements.

The basic equations are

$$\int_A \sigma \, dA = P \tag{4}$$

and

$$\int_A \sigma y \, dA = M_i . \tag{5}$$

As shown in Fig. 3, y is the distance of a finite element area dA from the bending axis and σ is the stress in this element. P is the applied thrust and M_i the internal moment. The stress at each element is a function of strain, ϵ, and therefore the stress-strain relationship must be defined first. Generally, the monotonic stress-strain relationship can be described well by the data obtained

from a tension specimen test, and recorded or represented by a mathematical equation as

$$\sigma = f(\epsilon) \tag{6}$$

However, if the stress-strain relationships are history-dependent, or if the strain reverses, Eq. (6) is invalid. In this study, the incremental stress-strain relationship is shown in Fig. 4, and defined as

$$\begin{aligned} \sigma &= f(\epsilon) && \text{for} \quad \epsilon = \epsilon^*, \\ \sigma &= \sigma^* - 2f\left(\frac{\epsilon^* - \epsilon}{2}\right) && \text{for} \quad -\epsilon \leqq \epsilon \leqq \epsilon^*, \\ \sigma &= -f(|\epsilon|) && \text{for} \quad \epsilon < -\epsilon^*, \end{aligned} \tag{7}$$

in which σ^* and ϵ^* are the largest compressive stress and strain to which the material of any element has been subjected. (The sign convention used here is plus for compression, and minus for tension.)

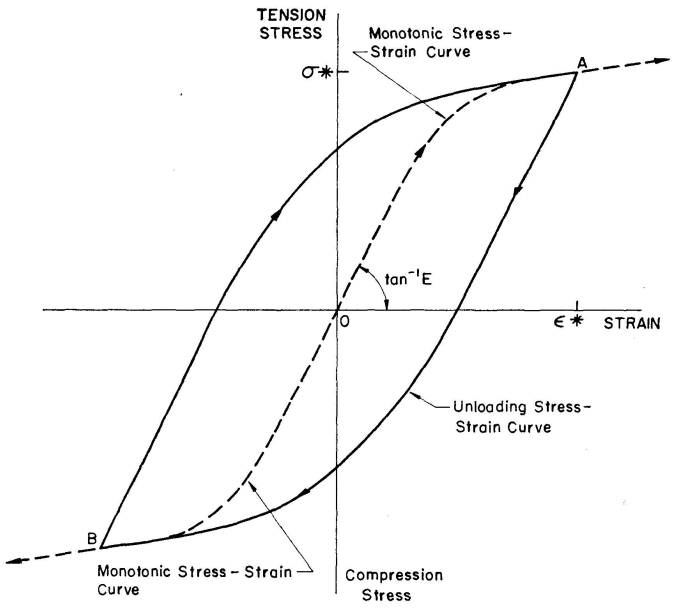

Fig. 4. Unloading Stress-Strain Curve.

The total strain at any point in a loaded beam-column is composed of a residual strain, ϵ_r, a constant strain over the entire cross-section due to the presence of thrust, ϵ_c, and the strain due to curvature, ϵ_ϕ. That is

$$\epsilon = \epsilon_r + \epsilon_c + \epsilon_\phi . \tag{8}$$

Here

$$\epsilon_\phi = y\phi , \tag{9}$$

where ϕ is the curvature at the section under consideration. When the stress-strain relationship is known, it is obvious that if P is specified, and by assuming a value for the curvature ϕ, the corresponding M_i can be determined by satisfying both Eqs. (4) and (5). If the thrust is applied first on the member and held constant through the whole loading process, a moment-curvature relationship can be established.

The numerical procedure for the determination of the moment-thrust-curvature curve is a trial- and error process [11]. For a given residual stress distribution, ϵ_r is known; and for the given curvature ϕ, ϵ_ϕ is known. By assuming an ϵ_c value for the whole cross-section, the total strain, and therefore the stress at each element area is determined. The summation of total internal forces must be equal to the given P, otherwise ϵ_c must be revised until Eq. (4) is satisfied. Then, the corresponding M_i can be evaluated by means of Eq. (5). By increasing the value of ϕ and repeating the calculation, a complete moment-curvature relationship can be determined for a specified thrust, P.

In this study, the stress-strain relationship of the material and residual stress distribution is programmed in subroutine subprogram forms. Both the material properties and the strain reversal effect are included.

Strain Reversal Effect

Strain reversal is defined here as the unloading stress-strain relationship which is different from the monotonic stress-strain relationship, as shown in Fig. 4. (Usually, it is convenient to assume that strain reversal will be defined by the monotonic curve.)

In Fig. 5a, the progress of applied strain on a section for a given constant thrust is shown. There are basically two modes by which the strain reversal can influence the M-ϕ-P curves. First, as shown in Fig. 5b, if the $(\epsilon_p - \epsilon_{rc})$ line runs across the strain reversal zone (where ϵ_p is the strain at the proportional limit and ϵ_{rc} is the compressive residual strain at a point), or ϵ_c, the initial applied strain due to a given constant thrust, is larger than the smallest value of $(\epsilon_p - \epsilon_{rc})$, the strain reversal will affect the resulting M-ϕ-P curves. The region affected by strain reversal is shown as the shaded area in Fig. 5b. The second mode is when the curvature is very large, then the tensile strain near the convex side can be larger than that at the proportional limit, as shown in Fig. 5c. Then at further loading, reversed tensile strain influences the M-ϕ-P curves. A combination of these two modes of strain reversal is also possible, if the applied thrust is high and the curvature is large. However, it was found that only at extremely large curvature, will tensile strain reversal be effective.

From this observation, if the thrust ratio, P/P_y (P_y is the axial force corresponding to yield stress level), is less than $(\sigma_p - \sigma_{rc})/\sigma_y$, then the reversed strain does not affect the results since it is still within the elastic range, except when the curvature ratio (ϕ/ϕ_{pc}) is very large. However, when the applied thrust ratio is larger than $(\sigma_p - \sigma_{rc})/\sigma_y$, pronounced differences could occur if the strain-reversal effect is neglected. To demonstrate the effect of strain reversal, a set of curves is presented in Fig. 6. The section is a welded A 514 steel H-shape built-up from flame-cut plates. The M-ϕ-P curves were plotted for P/P_y varying from 0.5 to 0.9. It is clear that for P/P_y less than 0.7 (proportional limit σ_p/σ_y is 0.8 and maximum compressive residual stress $\sigma_{rc}/\sigma_y =$

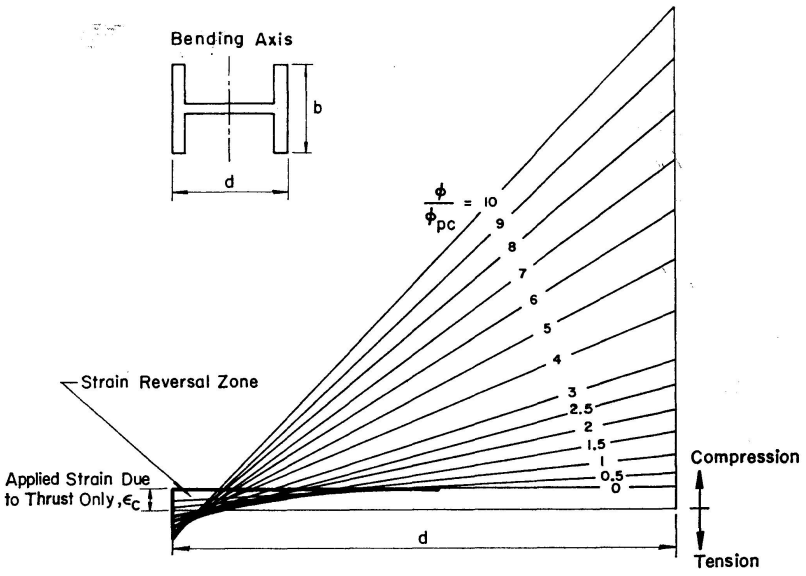

(a) Strain Diagram

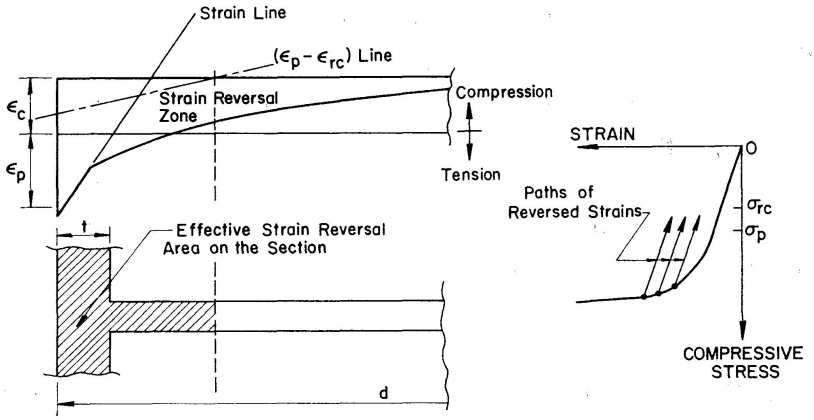

(b) Compressive Strain Reversal

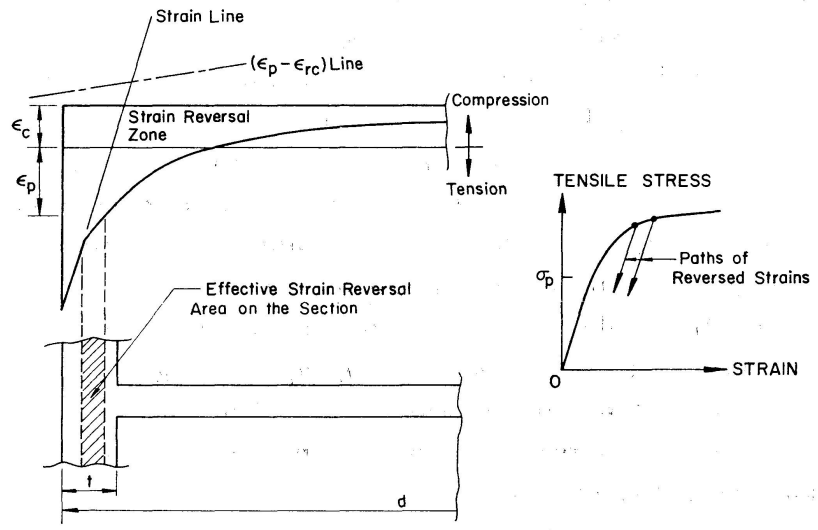

(c) Tensile Strain Reversal

Fig. 5. Typical Strain Diagram for a Beam-Column.

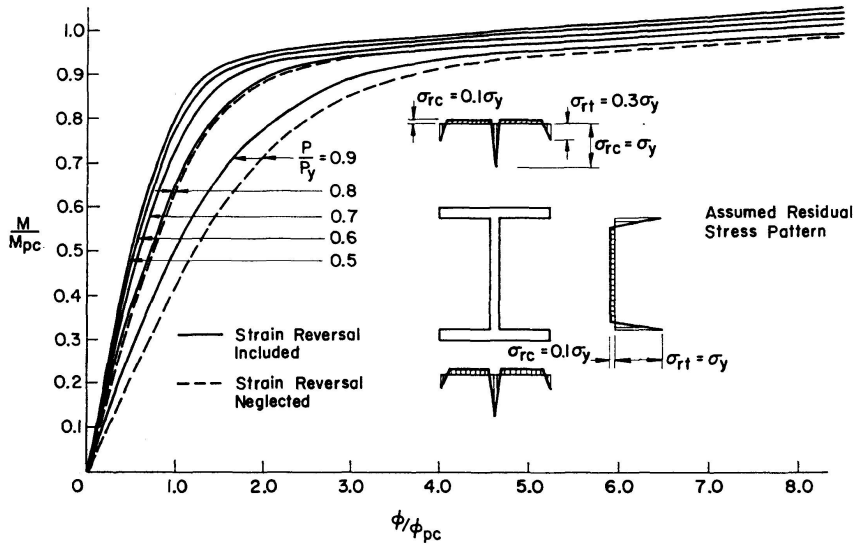

Fig. 6. Moment-Curvature-Thrust Relationship.

0.1), the case in which strain reversal is considered yields results in curves which are identical with the corresponding one in which the stress-strain relationship is assumed to follow the monotonic stress-strain curve only. However, for P/P_y equal to 0.8 and 0.9, significant differences are shown for the two cases. Therefore, the influence of strain reversal is pronounced and should be taken into account if the section exhibits a combination of compressive residual stresses and thrust which cause yielding immediately after thrust is applied.

Effects of Residual Stresses and Mechanical Properties

In addition to the consideration of the effect of strain reversal, the pattern of distribution and magnitude of residual stress also change the shape of the M-ϕ-P curve. Fig. 7 presents three types of residual stress distributions which represent the idealized residual stresses in (A) rolled low-carbon steel section, (B) rolled heat-treated A 514 steel section and (C) welded built-up A 514 steel shapes with flame-cut plates. If the mechanical properties are assumed to be elastic-perfectly plastic, the curves for the three types of residual stress distribution are curves (1), (2) and (4) in Fig. 7. It is noticed that there are significant differences among them in the elastic-plastic range. Generally speaking, the M-ϕ-P curve for the rolled structural-carbon steel section, which has the largest compressive residual stress ratio (σ_{rc}/σ_y) among the three, exhibits a smoother knee whereas the rolled heat-treated A 514 steel shapes, for which the compressive residual stress ratio is the smallest and thus residual stress effect the least, show a sharper knee.

Aside from the effect of residual stresses, the mechanical properties also play an important role in the M-ϕ-P curve; in Fig. 7, curves (2) and (3) are the M-ϕ-P curves for sections with identical residual stress distribution but

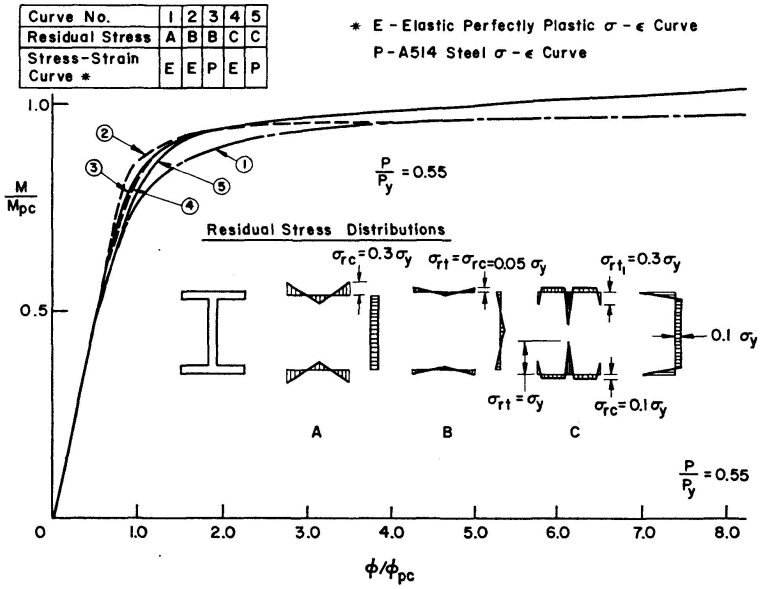

Fig. 7. Comparison of Moment-Curvature-Thrust Curves.

different mechanical properties; one is of elastic perfectly-plastic type and the other is representative of A 514 steel. For material with a non-linear type of stress-strain curve, such as that of A 514 steel, the M-ϕ-P curve is lower in the knee portion than that for which an elastic perfectly-plastic stress-strain curve is assumed. However, for curvature greater than that at the end of the knee, curve (3) is above curve (2), due to the strain-hardening property of the A 514 steel. Curves (4) and (5) are also presented in Fig. 7 for welding-type residual stresses and a similar behavior is observed.

For most practical beam-columns, the internal moments for a large portion of the member are within the knee range of the M-ϕ-P curve during the loading process. Therefore, the shape of the knee has a pronounced influence on the load-deformation relationship and the ultimate strength of the beam-columns. This leads to the emphasis on the basic assumptions of the residual stress distribution as well as of the shape of the stress-strain curve and of the strain-reversal phenomenon in the case when thrust is applied first and yielding occurs before the application of moment. The assumption that thrust is applied before the moment approximates the actual behavior of multi-story frames in which most of the axial forces in the columns are due to the dead load, and moments to the live load.

3. Load-Deflection Relationship

In the general practice for the design of planar structures it is often sufficient to know the ultimate strength of a beam-column. However, in plastic design, especially for multi-story buildings, it is necessary to determine the maximum moment of a joint of a subassemblage [12]. Therefore, not only the ultimate

moment capacity but also the complete load-deformation curve of each individual beam-column must be known. The most practical and useful way of presenting the load-deflection relationship of a beam-column is the end moment vs. end rotation curve.

There are generally two types of numerical integration for the determination of load vs. deformation curves of a beam column. One of the two methods is Newmark's numerical integration procedure [13]. The merit of Newmark's method is that it can be applied to any kind of end conditions and the interative process converges reasonably fast. However, Newmark's numerical integration diverges if the assumed end moment is larger than the ultimate load, and the descending branch of the M-θ curve becomes very difficult to obtain. The other numerical method is the so-called "stepwise" integration procedure [14]. This method has been used extensively in the development of column deflection curves (CDC's). However, during the construction of these CDC's it was assumed that reversed internal moments would still follow the monotonically increased M-ϕ-P curve. Therefore, end moment vs. end rotation (M-θ) curves obtained from these CDC's do not include the unloading effect. If this unloading effect is to be considered, then at each integration station of the beam-column the present moment must be compared with its history to determine the corresponding curvature. Consequently, if a series of CDC's are to be developed in the same manner, the location of the segment (which corresponds to a particular beam-column) of a CDC must be known beforehand

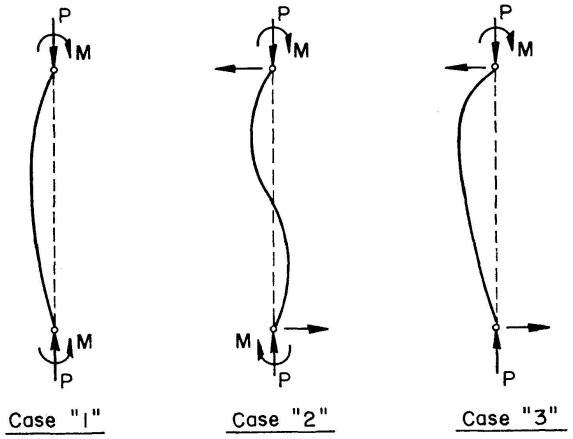

Fig. 8. Loading Conditions for Beam-Columns.

so that the history of CDC's can be made identical to that of the beam-column in question. This is impossible for most cases except for a few particular end-loading conditions as shown in Fig. 8; (1) equal end moments (single curvature), where the mid-height of the beam-column is always at the peaks of the CDC's, or (2) equal end moments (double curvature) and (3) one end pinned (zero end moment) where for case (2) the mid-height and for case (3) the zero moment end are always at one end of the CDC's. Therefore, integration of CDC's for case (1) can always be initiated at the quarter points, where the slopes are

zero, and for cases (2) and (3), at the zero deflection point, and then the loading effect can be considered. Of course, this negates the advantage of using CDC's, that is, that they are assumed to be history independent and hence may be used for beam-columns of any end conditions and length.

Numerical Procedure

The unloading behavior of beam-columns can be included in the M-θ curve, if the following numerical integration procedure is employed.

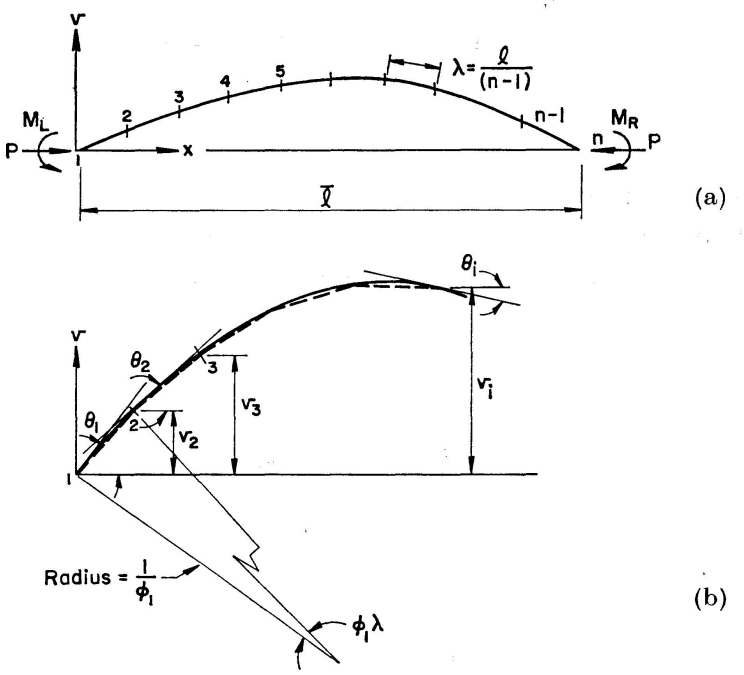

Fig. 9. Numerical Procedure for Calculating Load-Deflection Relationship.

1. Subdivide the length of the member which is under a constant thrust into n integration stations as shown in Fig. 9a. The distance between any two adjacent stations on the deflected member is $\lambda\,(=L/(n-1))$ (approximately equal to the arc length within the segment).
2. Assume that the segment in each sublength is a circular arc.
3. Assume an end rotation and an end moment at station 1.
4. Determine the curvature ϕ_1 at station 1 from the M-P-ϕ curve. (If present M_1 is less than the previous maximum M_1, the unloading M-P-ϕ curve is to apply.)
5. As shown in Fig. 9b, deflection at station 2, $v_2=\lambda \operatorname{Sin}(\theta_1-1/2\,\phi_1\lambda)$, and the slope at station 2, $\theta_2=\theta_1-\phi_1\lambda$.
6. And the moment at station 2 is $M_2=M_1+P\,v_2-\dfrac{M_1-M_n}{L}\cdot \operatorname{Cos}(\theta_1-1/2\,\phi_1\lambda)$.
7. Determine ϕ_2 from the M-P-ϕ curve, and continue the integration in the same manner as from step (4) to (6). That is,

$$v_i = \lambda \operatorname{Sin}(\theta_{i-1} - 1/2\,\phi_{i-1}\lambda) + v_{i-1},$$
$$\theta_i = \theta_{i-1} - \phi_{i-1}\lambda,$$
$$M_i = M_{i-1} + P\,v_1 - \frac{M_1 - M_n}{L}\lambda \sum_{2}^{i=1} \operatorname{Cos}(\theta_{i-1} - 1/2\,\phi_{i-1}\lambda).$$

8. If the assumed M_1 and θ_1 are correct, then at the nth station, v_n should be zero, or equal to a given value if sidesway of the beam-column is allowed. Otherwise M_1 must be decreased or increased if v_n is smaller than or larger than the given end deflection, and steps (3) to (7) repeated until v_n is within a certain allowable error.
9. Increase θ_1 and increase or decrease M_1 a certain amount and repeat the whole process from step (1) to step (8) until the complete M-θ as needed is obtained.

The numerical integration procedure suggested above is essentially the same as that used in the development of CDC's. The point of difference is the fact that the integration is carried out on the deflected shape of the member for fixed stations. Thus the history of every station can be recorded, and the unloading effect can be taken into account.

Unloading Effect

The M-θ curve for the equal end moments (single curvature) case is considered here. For this particular situation, the slope at the mid-height point is always zero and the internal moment at this point always increases during the whole loading history. Numerical integration can be simplified by starting at the mid-height point and working toward the end with only one half of the member [15]. The example given here is for the M-θ curves of A 514 steel; residual stresses of both the rolled and welded type are considered.

The actual moment-curvature relationship for an A 36 steel beam under reversed loading has been presented by Popov [16]. It was observed that when the moment is reversed, the initial unloading portion for a moment curvature hysteresis loop is approximately linear [16]. In the present study, elastic unloading of moment is postulated. The M-P-ϕ relationship is therefore represented by the following equations (see Fig. 10).

For $\phi = \phi^*$, $\phi = f(M_i, P)$,
$\phi < \phi^*$, $\phi = \phi^* - (M_i^* - M_i)/EI$.

Where ϕ^* and M_i^* are the largest curvature and internal moment, respectively, to which the column has been subject to any station.

The M-θ curves for A 514 steel beams-columns with slenderness ratios ranging from 20 to 40 are presented in Figs. 11 and 12. It is apparent that there is little difference between the M-θ curves including the unloading effect

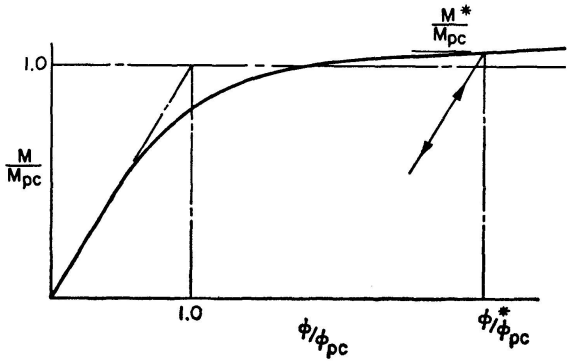

Fig. 10. Moment Curvature Curve with Unloading.

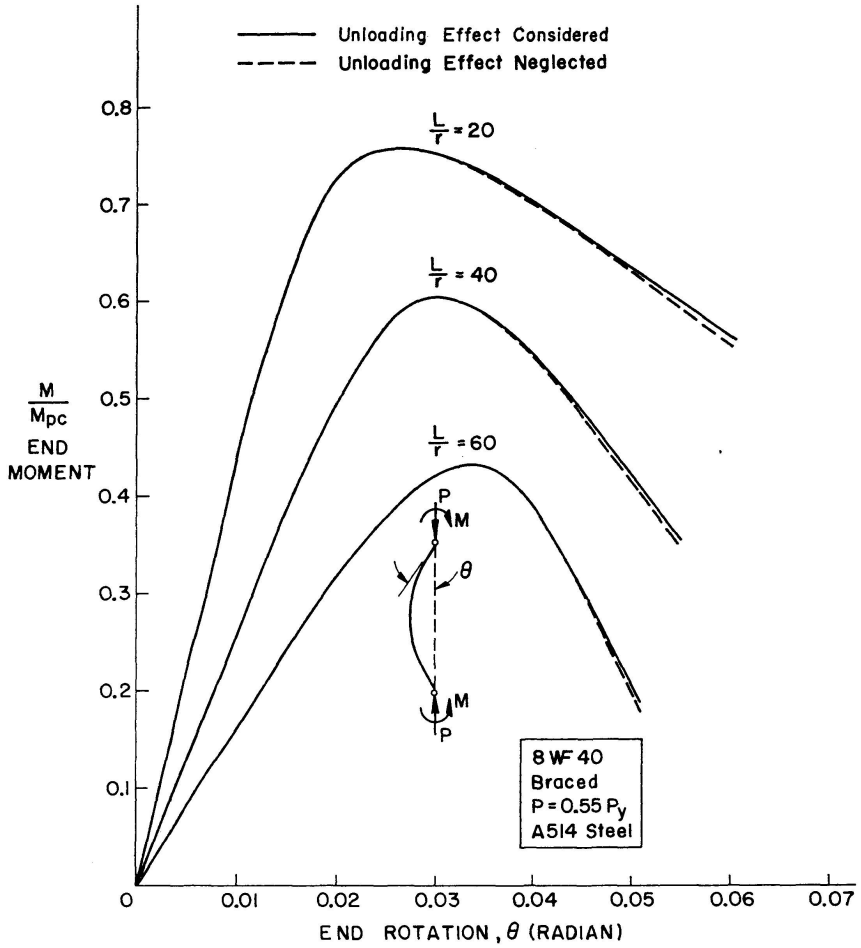

Fig. 11. End-Moment vs. End Rotation Curves.

and excluding it. The reasons for this are that the portions of the member that do unload are the less highly loaded regions, for example when $L/r = 20$, the moments at the unloading region are around $0.8\,M_{pc}$, which is approximately on the start of the knee of the M-P-ϕ curve where the elastic unloading effect is not pronounced, and also most of the deformation of the column continues to come from the regions under monotonic loading. From Figs. 10 and 11, it can also be seen that the unloading effect is more pronounced for low slenderness ratio columns whose ultimate strength is generally higher

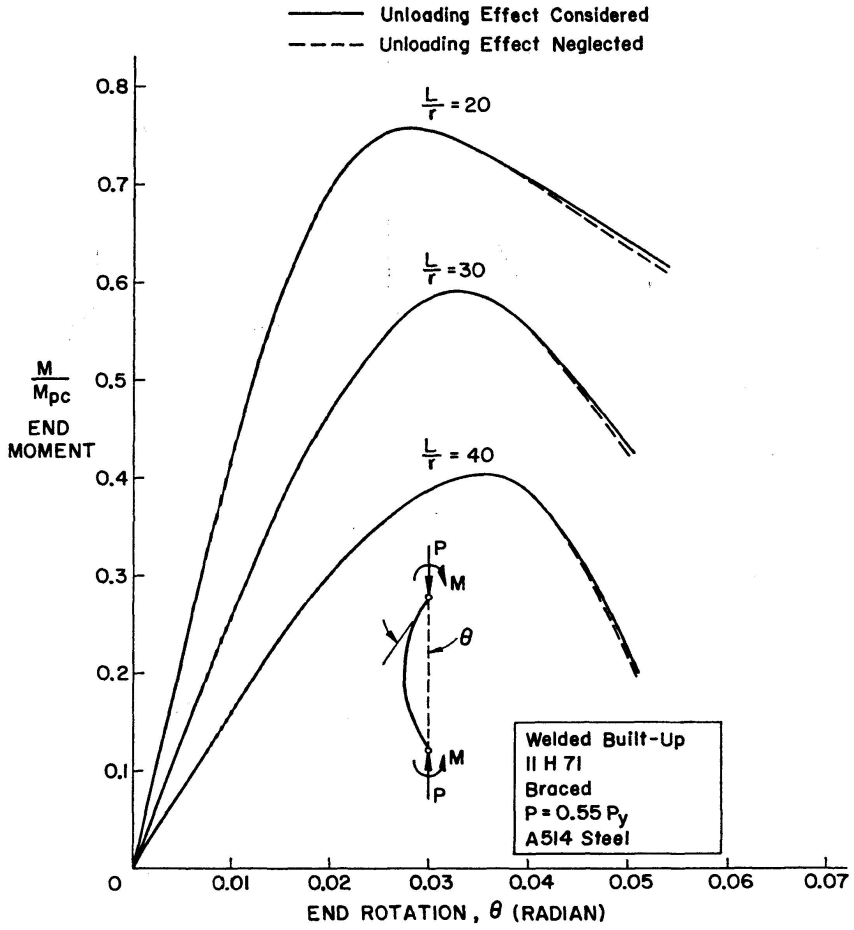

Fig. 12. End-Moment vs. End Rotation Curves.

than that of higher slenderness ratio columns. Also, on the descending portion of the M-θ curves, the larger the end rotation, the greater the difference between the loading and unloading curves.

Effects of Residual Stresses and Mechanical Properties

The effect of mechanical properties and residual stresses, as well as the unloading behavior, on the M-θ curves are important. In Fig. 13, the M-θ curves for columns with $L/r = 40$ are presented. The axial force is constant, $0.55 P_y$. The two patterns of residual stress shown in Fig. 2 are considered, that is, those for rolled shapes, and those for welded shapes with flame-cut plates.

It is seen that both the shape of the stress-strain curve and residual stress distribution can influence the M-θ curve. If the mechanical properties are kept the same, the difference can be approximately 10% in ultimate load if the patterns of residual stress are different. If nondimensional residual stresses are held constant, differences in the mechanical properties (stress-strain curve) can introduce a difference of up to 10% of the ultimate load. Therefore, accuracy

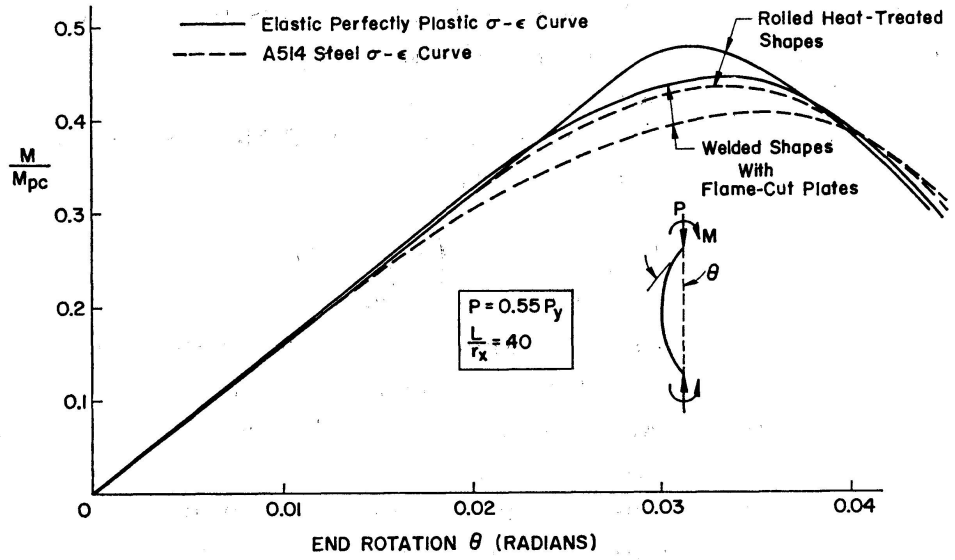

Fig. 13. Comparison of End-Moment and End-Rotation Curves.

of representation of both the stress-strain relationship of the material and the residual stress distribution in the section are needed in order to provide a good prediction of the strength of beam-columns.

Interaction Curves for A 514 Steel Beam-Columns

The interaction curves between P/P_y and M/M_p for equal end moment conditions (symmetrical bending) are shown in Fig. 14 for A 514 steel beam-columns with slenderness ratios equal to 20, 40, and 60. Beam-columns of rolled heat-treated shapes show higher ultimate strength than those of welded built-up shapes. This can be understood as the consequence of the smaller effect of residual stresses on the M-P-ϕ curves for rolled shapes than that for welded shapes.

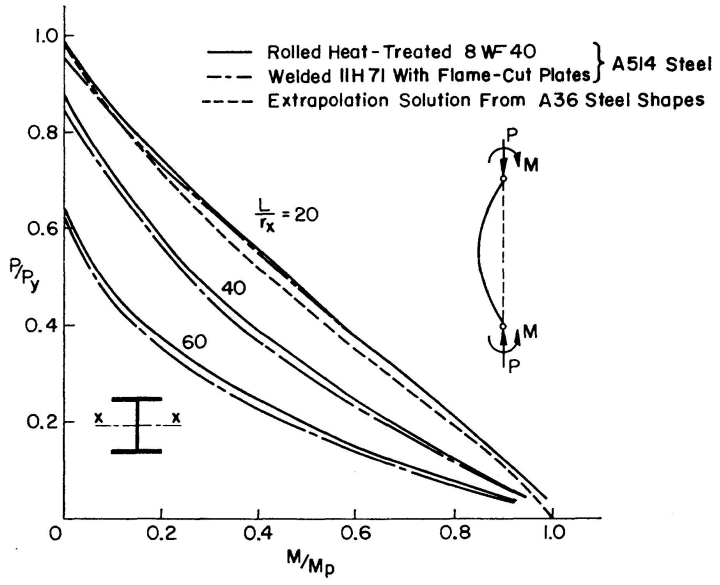

Fig. 14. Interaction Curves for A 514 Steel Beam-Columns.

The results obtained for A 514 steel beam-columns from direct interaction may be compared with the solutions extrapolating from the results obtained previously for A 36 steel beam-columns [12].

For beam-columns made of steel other than A 36, the slenderness ratio must be adjusted according to the following formula [12]:

$$\left(\frac{L}{r_x}\right)_{equivalent} = \left(\frac{L}{r_x}\right)_{\sigma_y} \sqrt{\frac{\sigma_y}{36}}.$$

The extrapolation solution sill be exact if the residual stress to yield strain ratio and the residual stress patterns are the same as those of rolled A 36 steel shapes, and if the stress-strain curve is elastic-perfectly plastic. For A 514 steel beam-columns these two conditions cannot be satisfied, and thus, yield only an approximate solution. The interaction curve determined from this extrapolation procedure is presented in Fig. 14 for the case $L/r_x = 20$. It is shown that the extrapolation solution is lower than the corresponding "exact solution".

4. Experimental Investigation

An experimental investigation of the behavior of beam-columns made of A 514 high strength constructional alloy steel has been carried out. The program consisted of tests of two full-scale beam-columns, one a rolled 8 WF 40 shape and the other a welded 11 H 71 shape (flame-cut plates). The members were tested in an "as-delivered" condition; no attempt was made to eliminate rolling or welding residual stresses by annealing. The magnitude and distribution of the residual stresses were determined by the method of "sectioning" [17], and it was found that they were close to the results of previous measurements [8], [9], [10] and hence the idealized residual stress distributions as shown in Fig. 2 were used for the theoretical predictions. The beam-columns were tested under equal end moment (single curvature) conditions.

Test Procedure

The procedure for testing beam-columns has been described in detail previously [4], [18] and only a brief outline is given here.

The general set-up of the beam-column specimen is shown in Fig. 15a. The horizontal moment arms are rigidly welded to the end of the column. The sizes of the beams are comparatively larger than that of the column so that the beam sections remain in the elastic range during the whole loading process. Pinned-end fixtures were utilized to ensure that there are no end moments other than those imposed by the moment arms, applied at the column ends. In Fig. 15a it can be seen that the axial force in the column is made up of the direct force applied by the testing machine, P and the jack force, F. To

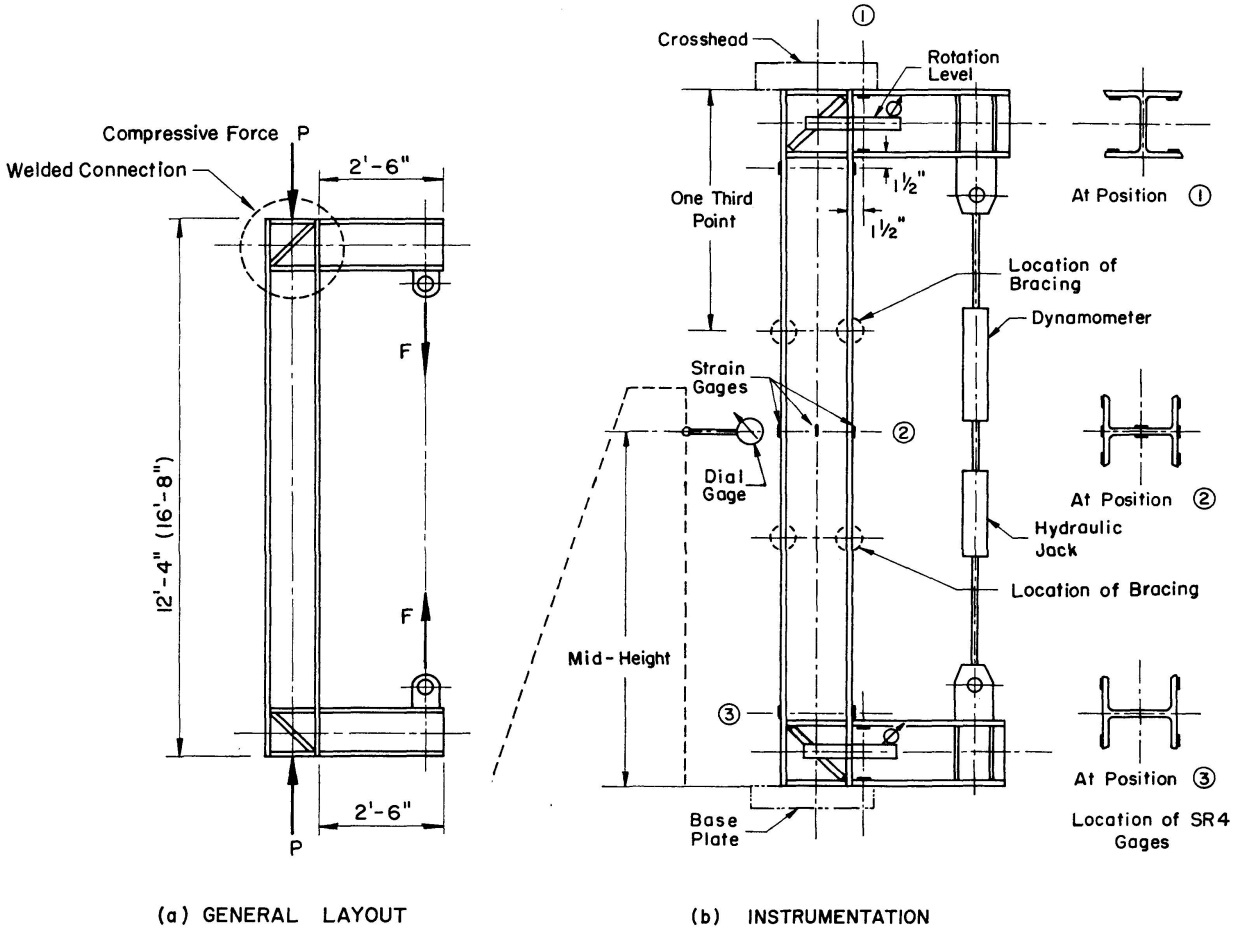

Fig. 15. Detail of the Beam-Column Specimen.

simulate the situation existing in the lower stories of a multi-story frame and to be in accord with the assumptions for the theoretical analysis, the tests were performed with the axial load held constant. Thus at each increment of load or deformation, the direct force, P, was adjusted so that the total force in the column remained at $0.55\,P_y$, where P_y is the yield load of the column.

The direct axial force, P, was first applied to the column; the beam-to-column joints were rotated by applying the jack force to the ends of the moment arms. The column was therefore forced into a symmetrical curvature mode of deformation. In order to preclude any deformation out of the plane perpendicular to the strong axis, the column was braced at the third points by two sets of lateral braces. The lateral braces used were designed for the laboratory testing of large structures permitted to sway [19]. In the early stages of loading, that is, in the elastic range, approximately equal increments of moment were applied to the column. In the inelastic range, comparatively larger deformations occur for the same amount of moment increment, therefore, end rotations instead of moment are used as a basis for loading in order to obtain a complete load-deformation curve with approximately evenly distributed test points.

At each increment of load or end rotation, the end rotations were measured by level bars (see Fig. 15b). The mid-height deflection, in the bending plane as well as out-of-plane, of the column was also measured by mechanical dial gages. SR-4 gages were mounted at the beam and column junctions as well as at several other locations along the column, as shown in Fig. 15b, to determine strain distribution in the column or to serve as a means for checking moments. Fig. 16 shows the photographs taken at the beginning and end of the test. The occurrence of local buckling of the compressed flange was determined by measuring the out-of-plane deformations of the flanges at five locations in the vicinity of mid-height of the beam-column with an inside micrometer.

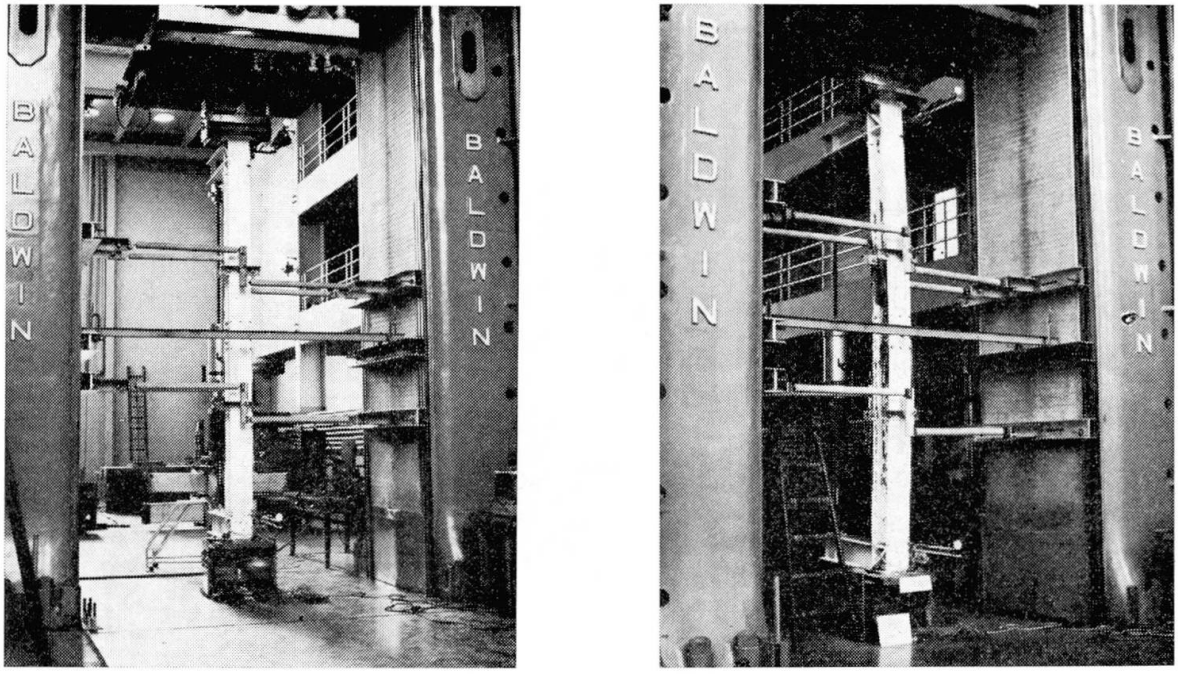

(a) Beginning of Test (b) End of Test

Fig. 16. Beam-Column in Testing Machine.

Test Results (In-Plane Behavior)

The results of the tests can best be presented in the form of end moment vs. end-rotation curves as shown in Figs. 17 and 18. In Fig. 17 the M-θ curve for the 8 WF 40 A 514 steel beam-column is shown. Fig. 18 contains the M-θ curve for the 11 H 71 welded A 514 steel beam-column. The moments indicated by open points represent the total applied moment determined from the hydraulic jack load. The length of the moment arm is the distance from the centerline of the column to the center of the rod to which the hydraulic jack is connected. The end moments are also checked by the reading of the dynamometer which is inserted in series with the jack and by four sets of SR-4 strain

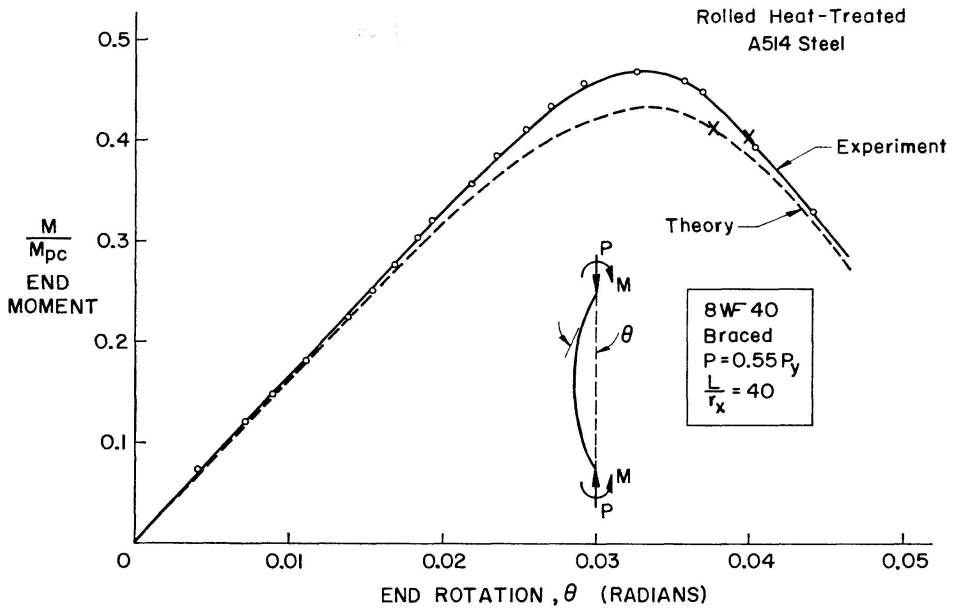

Fig. 17. Load-Deformation Relationship and Test Results.

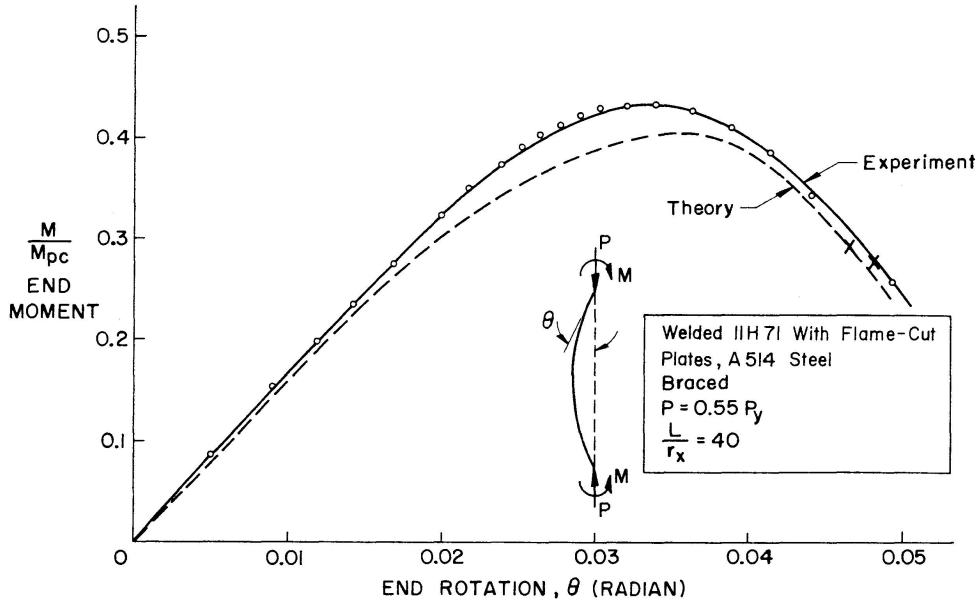

Fig. 18. Load-Deformation Relationship and Test Results.

gages which were affixed to the loading beam, near its junction with the column. The difference between the moment readings by these three means are shown in Fig. 19. It is apparent that they are rather consistent.

The length used to compute slenderness ratios of the columns were the distances between the points of intersection of the centerlines of the column and loading beams. For both beam-columns, the slenderness ratio, L/r, is 40. Comparison of the experimental results with the theoretical reveals that the testing points are above the theoretically obtained M-θ curve (Figs. 17 and 18). This discrepancy is due in part to the fact that the actual slenderness ratio

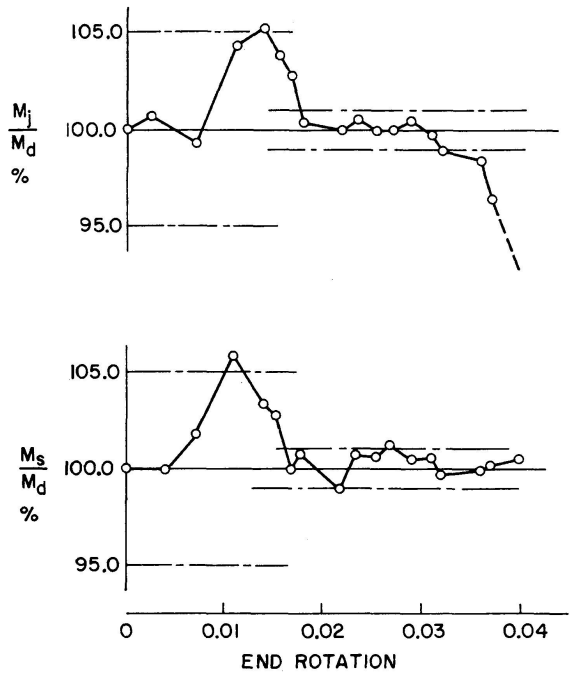

Fig. 19. Error of the Moment Readings.

has been reduced somewhat by the installation of joint stiffeners and to the fact that the actual stress-strain relationship determined from tension coupon tests shows a slightly higher proportional limit than that of the average typical stress-strain curve as shown in Fig. 1, on which the theoretical analysis was based. The tests are compared also to the theory in a plot of M/M_{pc} vs. L/r_x as shown in Fig. 20. The difference between theory and tests is approximately 6% of the theoretical prediction for both rolled and welded built-up shapes. From Fig. 20, it can also be observed that the difference of ultimate strength

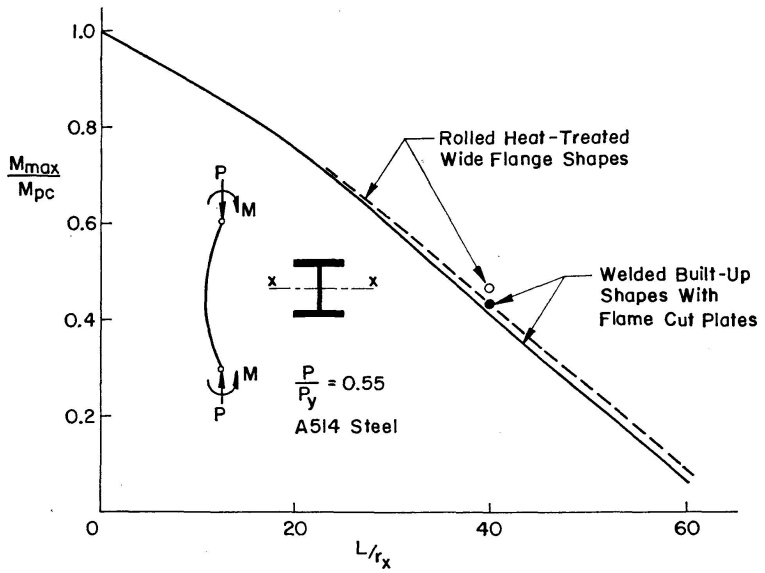

Fig. 20. Comparison Between Test Results and Theoretical Solutions.

for rolled and welded shapes vanished for low slenderness ratios. This is apparently because of the fact that the internal moments in the greater portion of the member are within the strain hardening region at ultimate load, and hence the residual stress effect becomes insignificant.

Test Results (Local Buckling)

The local buckling deformations of the flanges of the beam-columns were measured during the process of testing. It was observed that hardly any web buckling occurred, and that the b/t ratio of the flange provided sufficient stiffness to ensure the development of rotation capacity of the beam-column. That is, the local buckling of the flange occurred after the moment capacity had dropped five percent below its maximum value (ultimate strength).

It is difficult in general to analyze the buckling of plates in which residual stresses exist. The local buckling problem of columns or beam-columns with residual stresses becomes more involved because not only the compressive residual stresses could induce yielding before the local buckling stress is reached, but also because of the uncertainty of the coefficient of restraint at the junction of component plates [15]. In the case of H-sections, it was found that the assumption that the flange is divided into two cantilevers which have full deflection restraint but zero rotation restraint is close to reality, although conservative [20]. In this study, this same restraint condition was assumed for the flange of the beam-columns. It is not intended to perform an elaborate theoretical analysis with respect to the local buckling behavior of columns or beam-columns here. Experimental results are compared to the theoretical analyses available for the purpose of determining the maximum allowable b/t ratio for the flange, such that local buckling does not occur before the attainment of yield stress and for the prediction of the local buckling point for a beam-column. Reference 21 presents the theoretical and experimental investigations of the plate buckling under different edge conditions and residual stress patterns. Fig. 21 shows a plot of $\frac{\sigma_{cr}}{\sigma_y}$ vs. $\frac{b}{2t}\sqrt{\frac{\sigma_y}{E}}$ curves for plates simply supported and free at unloaded edges, and simply supported on both loading edges. Here, b and t denote the width and the thickness of the plate, respectively. Even though the stress-strain law, elastic perfectly-plastic, and residual stress patterns used in Ref. [21] are different from those used in this study, the solutions may provide a reasonable theoretical prediction for the buckling of A 514 steel plates in the determination of the critical b/t ratio. Fig. 21 shows that, even when the pattern of residual stress varies, the maximum $\frac{b}{2t}\sqrt{\frac{\sigma_y}{E}}$ values when $\frac{\sigma_{cr}}{\sigma_y} = 1.0$ are nearly the same, approximately equal to 0.45. It is therefore assumed that the maximum allowable b/t ratio for a yielded flange would be

$$\left(\frac{b}{2t}\right)_{max.} = 0.45 \times \sqrt{\frac{E}{\sigma_y}}.$$

For A 514 steel with $E = 29 \times 10^3$ ksi, $\sigma_y = 110$ ksi.

$$\left(\frac{b}{t}\right)_{max.} = 14.5,$$

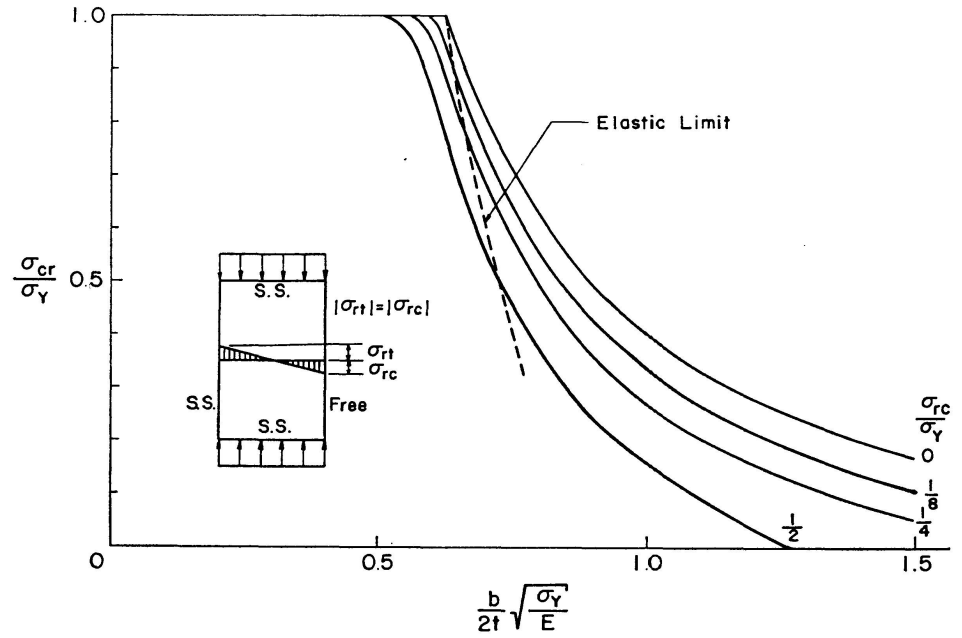

(a) With Residual Stress of Cooling Pattern

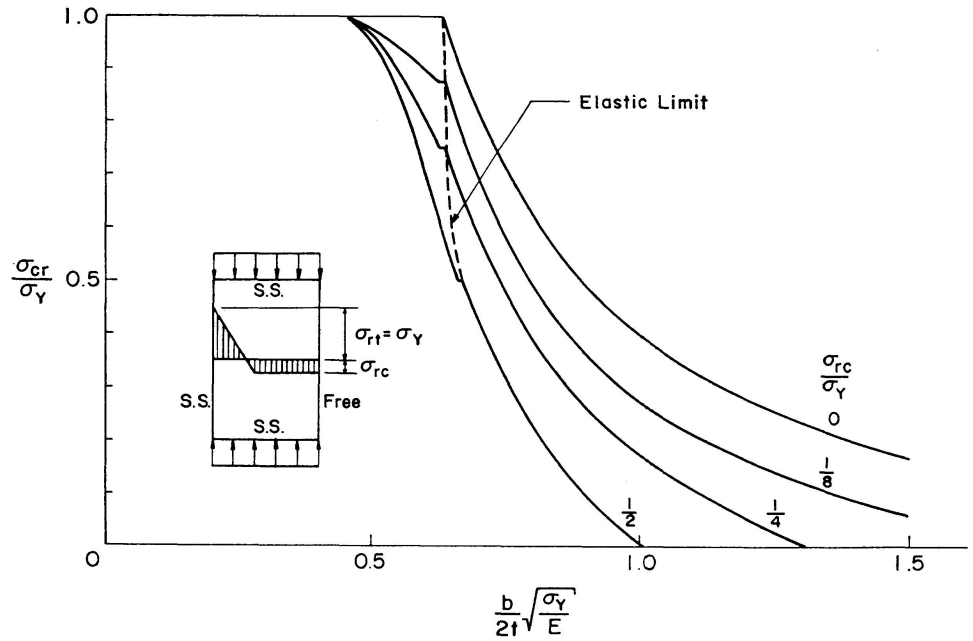

(b) With Residual Stress of Welding Pattern

Fig. 21. Plate Buckling Curves (Plates Simply Supported and Free at Unloading Edges).

where b and t are the width and thickness of the flange, respectively. The b/t ratio of both sections tested are equal to 14.35 which is slightly less than the maximum b/t for a yielded flange.

In order to have some experimental verification of the approximate critical b/t ratio determined and, in addition, to furnish some data relating mechanical properties, stub columns cut from the same pieces which also provided the beam-column specimens were tested under uniform axial load. The critical

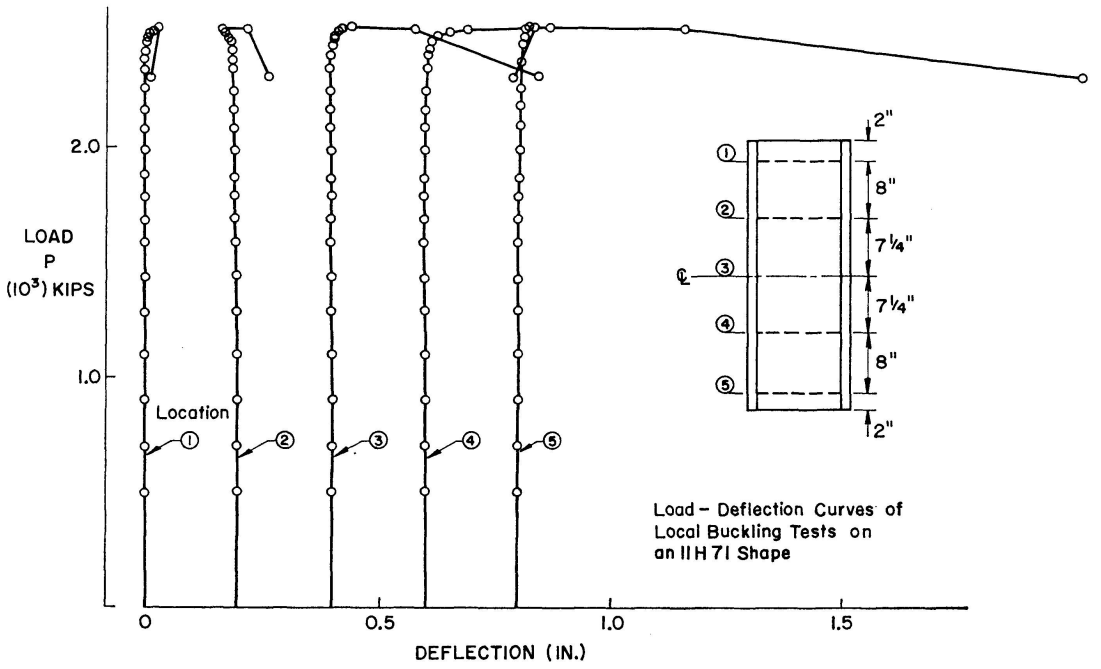

Fig. 22. Load-Local Deformation Curves.

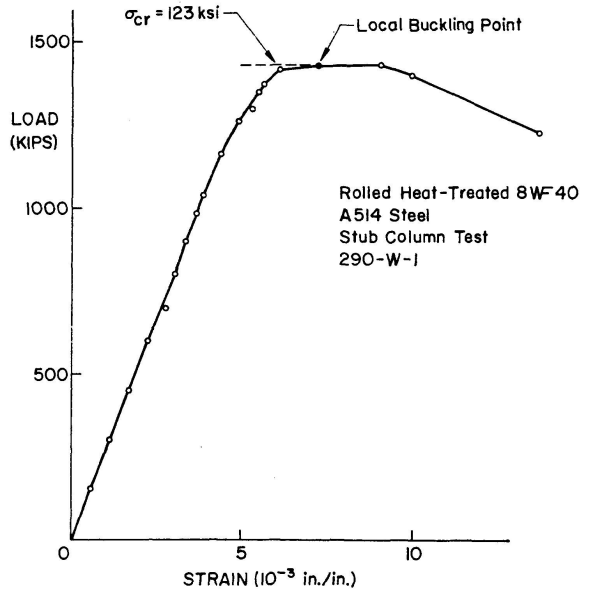

Fig. 23. A Stub Column Test.

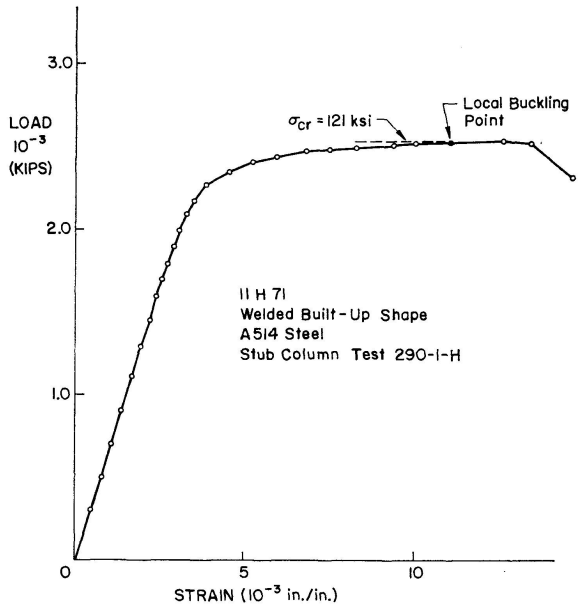

Fig. 24. A Stub Column Test.

local buckling strains were determined experimentally by the so-called "top of the knee method" [22]. Fig. 22 shows the load vs. out-of-plane deflection curves of the flange plates at several measured points. Then, the critical local buckling strain were determined as shown in Figs. 23 and 24 as the solid points. For both cases, the flange buckling stress or critical stress, σ_{cr}, is approximately equal to the yield stress of the section. Therefore, it seems reasonable to put $b/t = 14.5$ as the maximum allowable width-thickness ratio (or critical width-thickness ratio) if the flange is to be designed to withstand the yield load, P_y, without local buckling.

Theoretically, if the critical stress is equal to the yield stress, the critical strain, ϵ_{cr}, is equal to the sum of the strain at the yield point and the maximum tensile residual strain. That is

$$\epsilon_{cr} = 1.52\,\epsilon_y + \epsilon_{rt} = 0.006$$

for rolled heat-treated shapes,

and

$$\epsilon_{cr} = 3.04\,\epsilon_y = 0.0115$$

for welded built-up shapes. The stub column tests show that the critical strains are close to these values (Figs. 23 and 24), and hence these two critical strains are taken as the standard for determining the local buckling of beam-columns if b/t is less than 14.5.

The plate buckling problems in the strain hardening range have been studied by HAAIJER [23], and extended by LAY [20] for application to beam, beam-column and column members. Lay stated "Local buckling will not be critical until a critical region is strain-hardened", and adopted an aspect ratio, L/b, of 1.2 as the minimum criterion for local buckling where L is the half wave-length of the local buckle and b is the width of the flange. In this study the same $L/b = 1.2$ is used for the determination of local buckling point on the theoretical M-θ curve. It is taken as the local buckling moment when the minimum applied strain in a length of $1.2\,b$ is equal to the critical strain. For beam-columns with thin component plates, it is generally sufficient for the prediction of local buckling to assume that the strain applied to the flange is uniform across the thickness and width if the beam-columns are bent about the strong axis. For beam-columns with equal end moments which cause symmetrical bending, the local buckling point can be determined theoretically as an end rotation at which the strain at the location $0.6\,b$ from the mid-height reaches the critical strain. The experimental local buckling point was determined again by the "top of the knee" method. In Figs. 17 and 18, local buckling points are shown as cross marks. It is observed that there is good correlation between the local buckling points determined theoretically and experimentally. Also, it is interesting to notice that for welded built-up shapes the occurrence of local buckling is at a comparatively larger end rotation than that for rolled heat-treated shapes. Apparently, this is because of the higher tensile residual

stresses in the welded shape which increase the value of the critical strain necessary to cause total yielding of the flange. This indicates that welding residual stresses can actually increase the rotation capacity of the beam-column, if the termination of rotation capacity is taken as the local buckling point.

Furthermore, the initiation of local buckling does not seem to reduce to strength of beam-columns dramatically. The M-θ curves still follow their original path for some distance until pronounced out-of-plane deflections of the flanges are observed. If further study on the post local buckling behavior confirms this in the future, the use of beam-columns may be extended beyond the local buckling point.

5. Conclusions

The strength of rolled and welded H-shaped beam-columns made of A 514 steel has been investigated both theoretically and experimentally. The effect of the residual stresses due to cooling after welding or rolling, and the effect of strain reversal and of the mechanical properties of the steel are included in the determination of moment-curvature-thrust relationships. The load-deformation behavior of beam-columns was studied by carrying out numerical integration on fixed stations of the deflected shapes of the beam-columns; thus, the unloading effects due to reversed curvatures can be included. A computer program was developed to perform the computation.

Based on this study, the following conclusions may be made:

1. The mechanical properties of the material, the pattern and magnitude of residual stresses, and the strain reversal effect, all are important in the final shape of M-P-ϕ curves, which, in turn, are the sole basis for the determination of the load-deformation characteristics of beam-columns.
2. For beam-columns, the effect of strain reversal (that is, consideration of the unloading stress-strain relationship) is more pronounced for non-linear materials than for linear materials if other conditions, that is, residual stresses and thrust, are identical.
3. Consideration of the unloading effect generally is not pronounced immediately after the ultimate load. Significant differences between the inclusion and the exclusion of the unloading effect can be shown only at large rotations of the descending part of the moment-rotation curve. Thus, for simplicity, the unloading stress-strain relationship may be assumed identical to that for loading.
4. Two full scale beam-column tests, one a rolled 8 WF 40 shape and the other a welded 11 H 71 shape were conducted. A comparison between the theoretical curves and the corresponding experimental M-θ curves showed that the theory can predict not only the ultimate strength but also the complete history of a beam-column with good accuracy.

5. Comparing the direct integration solutions of this study to the extrapolation solutions obtained from previous investigations in A 36 steel shapes, it is shown that for A 514 steel shapes, both rolled and welded built-up, the direct integration solutions provide a higher ultimate strength. Hence, the extrapolation procedure may provide an approximate but conservative estimate of the strength of A 514 steel shapes.
6. The local buckling point of beam-columns was determined both experimentally and theoretically. It was found that the "regional criterion" provides a sufficient basis for the prediction of flange local buckling of beam-columns bent with respect to the strong axis, and that the stub column tests supply vital data for the determination of critical strain when the compression flanges buckle locally.

6. Nomenclature and Definitions

A	Area of cross section
b	Width of flange
d	Depth of section
E	Modulus of elasticity
E_{st}	Strain-hardening modulus
E_t	Tangent modulus
f	a function
I	Moment of inertia – subscripts x and y refer to the x and y axes (strong and weak axes), respectively
l	Chord length of a deflected member
M	Bending moment – subscripts R and L refer to moments at the right and left ends, respectively, of a beam-column, i refers to internal moment
M_p	Plastic moment
M_{pc}	Reduced plastic moment
M_u	Ultimate moment
P	Axial load
P_y	Axial yield load in a column
r	Radius of gyration – subscripts x and y refer to strong and weak axes radii
t	Thickness of flange
u, v, w	Displacement in the x, y, and z directions, respectively
x, y, z	Coordinate axes, coordinates of the point with respect to x, y, and z axes
ϵ	Strain
ϵ_c	Strain due to axial load
ϵ_{cr}	Critical strain
ϵ_p	Strain at proportional limit
ϵ_r	Residual strain

ϵ_{rc} Maximum compressive residual strain
ϵ_{rt} Maximum tensile residual strain
ϵ_{st} Strain at start of strain hardening
ϵ_t Total strain
ϵ_y Yield strain ($= \sigma_y/E$)
ϵ_ϕ Strain due to curvature
ϵ^* Largest strain any element area experienced
θ End rotation of a member
λ Slenderness function, distance between two adjacent integration stations
$\sum$ Summation
ϕ Curvature
ϕ_p Curvature at M_p
ϕ_{pc} Curvature at M_{pc}
σ Stress
σ_{cr} Critical stress
σ_p Stress at proportional limit
σ_r Residual stress
σ_{rc} Maximum compressive residual stress
σ_{rt} Maximum tensile residual stress
σ_y Yield stress (determined by 0.2% offset method for non-linear stress-strain relationship)
σ^* Largest stress any element area experienced

WF Rolled wide-flange shape
H Welded H-shape

7. Acknowledgements

This investigation was conducted at the Fritz Engineering Laboratory, Department of Civil Engineering, Lehigh University, Bethlehem, Pennsylvania.

The United States Steel Corporation sponsored the study, and appreciation is due to Charles G. Schilling of that corporation who provided much information and gave many valuable comments. Column Research Council Task Group 1, under the chairmanship of John A. Gilligan, provided valuable guidance.

References

1. Galambos, T. V., and Ketter, R. L.: Columns under Combined Bending and Thrust. Transactions ASCE, Vol. 126, Part 1, 1961, p. 1.
2. Ketter, R. L.: Further Studies on the Strength of Beam-Columns. Journal of the Structural Division, ASCE, Vol. 87. No. ST 6, Proc. Paper 2910, August, 1961, p. 135.
3. Ojalvo, M., and Fukumoto, Y.: Nomographs for the Solution of Beam-Column Problems. Bulletin No. 78, Welding Research Council, 1962.

4. VAN KUREN, T. C., and GALAMBOS, T. V.: Beam-Column Experiments. Journal of the Structural Division, ASCE. Vol. 90, No. ST 2, Proc. Paper 3876, April, 1964, p. 233.
5. LU, L. W., and KAMALVAND, H.: Ultimate Strength of Laterally Loaded Columns. Journal of the Structural Division, ASCE, Vol. 94, ST 6. Proc. Paper 6009, June, 1968.
6. YU, C. K.: Inelastic Columns with Residual Stresses. Ph. D. Dissertation, Lehigh University, Bethlehem, Pa., April, 1968. University Microfilms, Ann Arbor, Michigan.
7. American Society for Testing and Materials. ASTM Standards, Part 3, A 370–617, 1961.
8. ODAR, E., NISHINO, F., and TALL, L.: Residual Stresses in "T-1" Constructional Alloy Steel Plates, WRC Bull. No. 121, April, 1967.
9. ODAR, E., NISHINO, F., and TALL, L.: Residual Stresses in Welded Built-Up "T-1" Shapes. WRC Bull. No. 121, April, 1967.
10. ODAR, E., NISHINO, F., and TALL, L.: Residual Stresses in Rolled Heat-Treated "T-1" Shapes. WRC Bull. No. 121, April 1967.
11. PARIKH, B. P.: Elastic-Plastic Analysis and Design of Unbraced Multi-Story Steel Frames, Ph. D. Dissertation. Lehigh University, Bethlehem, Pa., 1966, University Microfilms, Ann Arbor, Michigan.
12. DRISCOLL, G. C., JR., et al.: Plastic Design of Multi-Story Frames. Notes on Plastic Design of Multi-Story Frames. Lehigh University, Bethlehem, Pa., 1965.
13. GODDEN, W. G.: Numerical Analysis on Beam and Column Structures. Prentice-Hall Inc., Englewood Cliffs, New Jersey, 1965.
14. OJALVO, M.: Restrained Columns, Proc. ASCE, 86 (EM 5), October, 1960.
15. TALL, L., Editor-in-Chief: Structural Steel Design. Ronald Press, New York, 1964.
16. POPOV, E. P. and FRANKLIN, H. A.: Steel Beam-to-Column Connections Subjected to Cyclically Reversed Loading. Preliminary Reports, 1965 Annual Meeting, Structural Engineer Association of California, February, 1966.
17. HUBER, A. N. and BEEDLE, L. S.: Residual Stress and the Compressive Strength of Steel. Welding Journal, Vol. 33, December, 1954.
18. LAY, M. G., AGLIETTI, R. A., and GALAMBOS, T. V.: Testing Techniques for Restrained Beam-Columns. Fritz Laboratory Report No. 270.7, October, 1963.
19. YARIMCI, E., YURA, J. A., and LU, L. W.: Techniques for Testing Structures Permitted to Sway. Experimental Mechanics, August 1967.
20. LAY, M.: The Static Load-Deformation Behavior of Planar Steel Structures. Ph. D. Dissertation, Lehigh University, Bethlehem, Pa., 1964. University Microfilms, Ann Arbor, Michigan.
21. NISHINO, F.: Buckling Strength of Columns and Their Component Plates. Ph. D. Dissertation, Lehigh University, Bethlehem, Pa., 1964, University Microfilms, Ann Arbor, Michigan.
22. HU, P. C., LUNDQUIST, E. E., and BATDORF, S. B.: Effect of Small Deviations from Flatness on Effective Width and Buckling of Plates in Compression. NACA, TN 1124, 1946.
23. HAAIJER, G.: Plate Buckling in the Strain-Hardening Range. ASCE Journal, Mechanics Division, Vol. 83, No. EM 2, April 1967.

Summary

The ultimate strength, load deformation behavior, and local buckling phenomena of welded and rolled ASTM A 514 steel beam-columns were investigated analytically and experimentally. Particular attention was paid to the influence of non-linearity in the stress-strain relationship of this heat-treated steel. The mechanical properties of the material, the pattern and magnitude of residual stresses, and the effect of strain reversal, all have an important influence on the behavior of the beam-columns.

Résumé

La résistance à la tension, le comportement de la déformation due à la charge ainsi que des phénomènes locaux de la résistance au flambage sur des colonnes en acier ASTM A 514 soudé et laminé fûrent examinés par voie analytique et expérimentale. Une attention particulière fût attribuée à l'influence de non-linéarité dans la relation charge/sollicitation dudit acier traité à chaud. Les propriétés mécaniques du matériel, les épreuves, le degré des sollicitations ainsi que l'effet d'une charge variable ont tous une influence importante sur le comportement des colonnes.

Zusammenfassung

Die Traglast, das Lastverformungs-Verhalten und die örtlichen Beulerscheinungen von druck- und biegebeanspruchten geschweissten und gewalzten ASTM-A 514-Profilen wurden analytisch und experimentell untersucht. Besondere Aufmerksamkeit wurde dem Einfluss der Nichtlinearität der Belastungsbeanspruchung dieses vergüteten Stahles gewidmet. Sowohl die mechanischen Eigenschaften des Materials, des Verlaufes und der Grösse der Eigenspannungen ebenso wie die Auswirkungen wechselnder Belastung haben alle bedeutenden Einfluss auf das Verhalten dieser Stützen.

Leere Seite
Blank page
Page vide